

# Theory of Electronic Raman Scattering in Disordered $d$ -wave Superconductors

T. P. Devereaux

*Department of Physics, University of California, Davis, CA 95616*

## Abstract

A theory for the effect of impurity scattering on electronic Raman scattering in unconventional superconductors is presented. The impurity dependence of the spectra can be used to distinguish between conventional (anisotropic  $s$ -wave) or unconventional ( $d$ -wave) energy gaps, and excellent agreement with the data on three cuprate superconductors is shown for  $d_{x^2-y^2}$  pairing. The full frequency dependence of the spectra can be reproduced by including inelastic scattering due to spin fluctuations and/or Coulomb scattering on a partially nested Fermi surface.

PACS numbers: 78.30.-j, 74.72.-h, 74.25.Gz, 74.20.Mn

By now a more coherent picture of the pair state symmetry in cuprate superconductors has emerged, and it has become increasingly evident that a gap with *predominantly*  $d_{x^2-y^2}$  pairing symmetry can provide an adequate description of many experiments [1]. However, the question remains or not whether the order parameter changes sign around the Fermi surface. The available data on Josephson junction and point-contact tunneling measurements seems to in favor of the former, although examples exist to the contrary [2,1]. In addition, it has been argued that the impurity dependence of certain correlation functions can be used to determine whether the gap changes sign. In particular, a detailed analysis has been given for the case of the electromagnetic penetration depth [3], and the crossover from  $T$  to  $T^2$  at a temperature  $T^*$  which grows with impurity concentration has been taken to support  $d$ -wave pairing. Similar considerations can be made for the Knight shift, NMR rates, etc. [1]. However, the evidence gained from the penetration depth or other correlation functions is incomplete in that only the topology of the energy gap nodes can be identified from the power-law behavior at low temperatures, which leaves the actual gap symmetry unspecified. For instance, in tetragonal superconductors, there are 5 pure representations,  $(d_{x^2-y^2}, d_{xy}, d_{3x^2-y^2}, d_{xz}$  and  $d_{yz})$ , which yield the same low temperature power-laws and impurity dependences for, e.g., the penetration depth, NMR rates, density of states, etc.

It has recently been shown that both the electronic and phonon contributions to Raman scattering in superconductors can be used to identify the order parameter symmetry and can distinguish between the various representations for  $d$ -wave pairing [4]. Raman scattering measures effective intracell density fluctuations  $\tilde{\rho}_{\mathbf{q}}$ ,

$$\tilde{\rho}_{\mathbf{q}} = \sum_{\mathbf{k}, \sigma} \gamma(\mathbf{k}) c_{\mathbf{k}-\mathbf{q}/2, \sigma}^\dagger c_{\mathbf{k}+\mathbf{q}/2, \sigma}, \quad (1)$$

where  $c_{\mathbf{k}, \sigma}^\dagger$  ( $c_{\mathbf{k}, \sigma}$ ) is the creation (annihilation) operator for an electron with wavevector  $\mathbf{k}$  and spin  $\sigma$ . For the case of non-resonant scattering [5], the Raman vertex  $\gamma$  is directly related to the curvature of the band dispersion  $\epsilon(\mathbf{k})$  and incident  $\mathbf{e}^{\mathbf{I}}$  and scattered  $\mathbf{e}^{\mathbf{S}}$  polarization light vectors via

$$\gamma(\mathbf{k}) = \frac{m}{\hbar^2} \sum_{\mu,\nu} e^I_\mu \frac{\partial^2 \epsilon(\mathbf{k})}{\partial k_\mu \partial k_\nu} e^S_\nu, \quad (2)$$

which can be expanded in terms of a complete set of orthogonal functions on the Fermi surface,  $\gamma(\mathbf{k}) = \sum_L \gamma_L \Phi_L(\mathbf{k})$ . For bands with non-parabolic dispersion, all  $L$  symmetry channels can in principle contribute to the vertex. Thereby, fluctuations on different parts of the Fermi surface can be selected by orienting the polarization light vectors.

It was shown in Ref. [4] that the symmetry- (polarization-) dependence of the Raman spectra straightforwardly arises through the coupling of the Raman vertex to an anisotropic energy gap. The main features of the theory for clean superconductors with  $d_{x^2-y^2}$  pairing symmetry are as follows: 1) due to the presence of the nodes, no clear gap threshold is seen for any polarization channel, 2) the peak in the spectra occurs at the largest frequency for polarizations which select the  $B_{1g}$  channel (i.e, for YBCO, crossed in-lane polarizations aligned 45 degrees with respect to the  $a-b$  axes), while lower peaks are observed in the  $B_{2g}$  (45 degree rotation of the  $B_{1g}$  orientation) and  $A_{1g}$  (mostly parallel polarizations) channels in descending order, respectively, and 3) the low frequency behavior is given by  $\omega^3$  for the  $B_{1g}$  channel, while is linear in  $\omega$  for the other channels. Such a strong polarization dependence of the spectra allowed for a stringent test of the predictions for  $d_{x^2-y^2}$  pairing, and good agreement of the theory was shown with the data on three cuprate materials,  $\text{YBa}_2\text{Cu}_3\text{O}_7$ ,  $\text{Bi}_2\text{Sr}_2\text{CaCu}_2\text{O}_8$ , and  $\text{Tl}_2\text{Ba}_2\text{CuO}_6$ .

However, like other correlation functions, only  $|\Delta(\mathbf{k})|$  could be determined from the fit, and thus it could not be ascertained whether the gap changed sign around the Fermi surface. In addition, the fit was less satisfactory for samples with increasing disorder, with the best agreement found for a sample of Bi 2:2:1:2 with a transition temperature  $\sim 86$  K. The theory also failed to predict *any* Raman intensity in the normal state due to phase space restrictions (consequence of the limit  $\mathbf{q} \rightarrow 0$ ), and a large and unspecified smearing width  $\Gamma \sim 0.2\Delta_0$  was needed even at low temperatures.

The purpose of this Letter is to show that impurity scattering can resolve the above deficiencies of the theory. The  $T$ -matrix approach to incorporate repeated scattering events

from a single impurity site has been well documented [6]. The two parameters to describe the theory are the cotangent of the scattering phase shift,  $c = \cot(\delta)$ , and the impurity concentration  $n_i$  described through the scattering rate  $\Gamma = n_i/\pi N_F$ , where  $N_F$  is the density of states per spin at the Fermi level. To maintain gauge invariance, the effects of impurity scattering are included into both the self energy and vertex renormalizations. The case for an even parity vertex (such as the Raman vertex) has been worked out for general pair-states under the assumption of particle-hole symmetry and s-wave impurity scattering in Ref. [6], and thus we can adopt these methods accordingly. For the case of the Raman vertex, impurity dressings are only important for the case of the density ( $L = 0$ ) channel, while other channels do not couple to the scattering. Since the density channels are completely screened out (intercell charge fluctuations) for vanishing momentum transfers, for our purposes we can set the vertex corrections to zero. This will not hold for an impurity interaction which is non-zero in other channels (i.e., a  $\mathbf{k}$ -dependent impurity interaction). This can be remedied by including couplings to other channels, but the analysis can not be carried as far analytically.

Our expression for the Raman response is then given by

$$\chi''(\mathbf{q} \rightarrow 0, i\Omega) = -T \sum_{i\omega} \sum_{\mathbf{k}} Tr \gamma(\mathbf{k}) \hat{\tau}_3 \hat{G}(k, i\omega) \hat{\tau}_3 \gamma(\mathbf{k}) \hat{G}(\mathbf{k}, i\omega - i\Omega), \quad (3)$$

where  $Tr$  denotes the trace,  $\hat{\tau}$  are Pauli matrices, and  $\gamma$  is the bare Raman vertex, Eq. (2). We use the standard weak coupling BCS Green's function dressed by the impurity self energy,

$$\hat{G}(\mathbf{k}, i\omega) = \frac{i\tilde{\omega} + \tilde{\epsilon}(\mathbf{k})\hat{\tau}_3 + \Delta(\mathbf{k})\hat{\tau}_1}{(i\tilde{\omega})^2 - \tilde{\epsilon}(\mathbf{k})^2 - \Delta(\mathbf{k})^2}, \quad (4)$$

where the tilde indicates the renormalized frequency and band energy via

$$\begin{aligned} i\tilde{\omega} &= i\omega - \Sigma_0(i\tilde{\omega}), \\ \tilde{\epsilon}(\mathbf{k}) &= \epsilon(\mathbf{k}) - \Sigma_3(i\tilde{\omega}). \end{aligned} \quad (5)$$

Lastly, the matrix self energy is given in terms of the integrated Green's function  $g(i\omega) = \frac{1}{\pi N_F} \sum_{\mathbf{k}} Tr \hat{\tau}_0 \hat{G}(\mathbf{k}, i\omega)$ ,

$$\hat{\Sigma}(i\omega) = \Gamma \frac{g(i\omega)\hat{\tau}_0 - c\hat{\tau}_3}{c^2 - g^2(i\omega)} = \Sigma_0\hat{\tau}_0 + \Sigma_3\hat{\tau}_3. \quad (6)$$

Our choice of the gap parameter is  $\Delta(\mathbf{k}) = \Delta_0 \cos(2\phi)$ , where we will for simplicity chose to work with a 2-D (cylindrical) Fermi surface.

The results of the theory with the inclusion of impurity scattering in the Born ( $c \gg 1$ ) and unitary ( $c = 0$ ) limits are shown in Figure 1. The impurity scattering smears out the sharp features of the spectra (i.e., the logarithmic divergence of the spectra at the gap edge for the  $B_{1g}$  channel) and thus can provide an explanation for the broadening seen in the data at low temperatures. In addition, the anisotropy of the peak positions is maintained (unless the scattering is so large that the normal state behavior is recovered). The coupling of the gap and Raman vertex lead to polarization dependent peak positions, with  $\omega_{peak}/\Delta_0 = 2.0, 1.8$ , and 1.2 for the  $B_{1g}, B_{2g}$ , and  $A_{1g}$  channels, respectively. Thereby, the channel which shows the peak at the highest frequency gives the predominant symmetry of the energy gap. This was used in Ref. [4] to conclude that the energy gap in the cuprates is *predominantly*  $d_{x^2-y^2}$  symmetry as opposed to  $d_{xy}$  or other  $d$ -wave representations.

To determine further whether the gap is *entirely* of  $d_{x^2-y^2}$  symmetry, the impurity dependence of the low frequency behavior of the channel dependent spectra can be exploited. From Figure 1, it is seen that Born impurity scattering yields low frequency exponents that are the same as for clean materials (unless of course  $\Gamma \sim \Delta_0$  and the normal state is recovered). However, in the unitary case, while the low frequency behavior remains linear in frequency in the  $A_{1g}$  and  $B_{2g}$  channels, below a characteristic frequency  $\omega^*$  the behavior changes from  $\omega^3$  to linear in  $\omega$  for the  $B_{1g}$  channel. This is due to a nonzero density of states at the Fermi level, which allows for normal-state-like behavior to be recovered [7]. As in the case of the penetration depth [3], the scale  $\omega^*$  grows with increasing impurity concentrations. However, the exponent is symmetry dependent (remains 1 for  $A_{1g}$  and  $B_{2g}$  channels, while *decreases* from 3 to 1 for the  $B_{1g}$  channel, which is unlike the penetration depth). This is in marked contrast to the impurity dependence of the spectra for anisotropic  $s$ -wave gaps, since in that case, the exponents for *all* channels would grow as the gap becomes more isotropic for

increased impurity scattering [8]. In particular, the impurity dependence of the  $B_{1g}$  channel is opposite to what one would expect if the gap was anisotropic  $s$ -wave. Thus the impurity dependence can be systematically checked to determine whether the gap has accidental or intrinsic zeroes, or more generally, if the gap is anisotropic  $s$ -wave with predominantly  $B_{1g}$  symmetry, or if it is  $d_{x^2-y^2}$  symmetry.

To make a comparison to experiment, we note that the impurity dependence, for instance via Zn doping, has not been systematically checked via Raman scattering for any of the cuprate superconductors. Raman scattering measurements of the electronic background have been performed on materials of varying quality. In particular, we focus on three materials, as-grown  $\text{Bi}_2\text{Sr}_2\text{CaCu}_2\text{O}_8$  ( $T_c = 86K$ ), oxygen-annealed  $\text{Bi}_2\text{Sr}_2\text{CaCu}_2\text{O}_8$  ( $T_c = 79K$ ) [9], and  $\text{Tl}_2\text{Ba}_2\text{CuO}_6$  ( $T_c = 80K$ ) [10]. The materials show polarization dependent spectra, with the peak positions accurately predicted using a gap of  $d_{x^2-y^2}$  symmetry (see Ref. [4]). These compounds differ with respect to both surface quality and the presence of bulk impurity defects. Fits using the theory for clean materials [4] required a Gaussian broadening width  $\Gamma \sim 0.2\Delta_0$ . Such large broadening, if attributed solely to impurity scattering, would of course also lead to a large reduction of  $T_c$ . However, the majority of the smearing could be due to a distribution of  $T_c$  values (of the order of 20 percent in Tl 2:2:0:1) and inelastic quasiparticle scattering, which could be taken into account via strong coupling theory. The actual magnitude of the scattering to be attributed to impurities remains an open issue which requires both a non-phenomenological theory to include the effects of inelastic scattering, doping, and disorder on the pairing interactions, as well as a systematic experimental analysis.

We present the comparison of the theory to the spectra obtained in Refs. [9,10] on the three compounds in Figure 2. The spectra shown in the Figure are for the  $B_{1g}$  and  $B_{2g}$  channels for both Bi 2:2:1:2 samples, and for  $B_{1g}$  and  $A_{1g}$  for Tl 2:2:0:1. The parameters used to fit the data are  $\Delta_0 = 287, 192, \text{ and } 240 \text{ cm}^{-1}$ , for the energy gap, and resonant impurity scattering rate  $\Gamma/\Delta_0 = 0.125, 0.2, \text{ and } 0.25$  for as-grown, oxygen-annealed Bi 2:2:1:2, and Tl 2:2:0:1, respectively. No Gaussian broadening was used. The theory shows

that the anisotropy of the peak positions is preserved even in the presence of impurity scattering which suggests that the gap anisotropy is robust to disorder. The linear rise in frequency of *both* the  $B_{1g}$  and  $A_{1g}$  channels is a direct consequence of resonant impurity scattering. This is shown in log-log plot of the low frequency part of the  $B_{1g}$  response for the three materials in the inset of Figure 2. Born scattering can not fit the data as the amount of scattering to produce the linear rise in the  $B_{1g}$  channel fully suppresses the peak feature. The crossover scale  $\omega^*$  grows with increasing disorder, which leads to a more pronounced linear rise of the  $B_{1g}$  channel. The crossover frequency is given by  $\omega^*/\Delta_0 = 0.38, 0.47$ , and  $0.73$  for the as-grown, oxygen-annealed Bi 2:2:1:2, and Tl 2:2:0:1, respectively. This is in consistent with the predictions of  $d$ -wave pairing and is difficult to reconcile using an anisotropic  $s$ -wave gap. Thus, this crucial issue merits a systematic experimental examination of the low frequency region of the spectra using greater resolution.

The theoretically predicted spectra fail to reproduce the flat background extending out to large Raman shifts [12] since the calculated spectra falls off as  $1/\omega$  [13]. “Marginal-like” behavior [14] can be phenomenologically modelled by inserting a self energy piece of the form

$$\Sigma''(\omega) = \alpha\sqrt{\omega^2 + \beta T^2}, \quad (7)$$

where  $\alpha$  and  $\beta$  are constants. This form for the self-energy arises in the normal state when electron-electron scattering on a nested Fermi surface is taken into account [15] or spin-fluctuation scattering is considered [16]. While the inclusion of this term to the self energy does not take the modifications of superconductivity into account and also neglects vertex corrections of the interactions, the flat behavior at high frequencies can be reproduced to fit the data. This is shown explicitly in Figure 3, which compares the results of the theory with and without the added self energy to the  $B_{1g}$  data on the annealed Bi 2:2:1:2 sample using a value of the gap,  $\Delta_0 = 190 \text{ cm}^{-1}$ . The parameters used are  $\alpha/\Delta_0 = 0.25$ ,  $\beta = 3.3$ , and small resonant scattering  $\Gamma = 0.01\Delta_0$  for the solid line, which is to be compared to the fit made in Figure 2 without the self energy term added (redrawn in Figure 3 as the dotted

line). While the low frequency portion of the spectrum  $\omega < 2\Delta_0$  is relatively unaffected, the higher frequency region is well fit by the self energy inclusion. It is expected that a better fit could be obtained when modifications due to superconductivity are included in the interaction self energy.

The agreement of the theory to the data leads to the following conclusions: First, the anisotropy of the peak positions result from a coupling of the Raman vertex to an energy gap with *predominantly*  $d_{x^2-y^2}$  symmetry. Second, since the spectra do not show evidence for a reorganization of states to higher frequencies with increasing disorder, and on the contrary, reorganize to lower frequencies, this strongly suggests that the gap therefore changes sign and has unconventional  $d_{x^2-y^2}$  symmetry as opposed to conventional anisotropic  $s$ -wave symmetry. This is seen from the increased prominence of the linear rise of the  $B_{1g}$  spectra and the increase of  $\omega^*$  for increasing resonant scattering. Lastly, the full frequency range of the spectra can be modelled by taking into account an additional interaction self energy. A systematic check of impurity scattering on a single compound would clarify these points further.

The author would like to thank D. Einzel, R. Hackl, P. Hirschfeld, D. Pines, R. R. P. Singh, D. Scalapino, R. T. Scalettar, A. Virosztek, A. Zawadowski, and G. Zimanyi for many enlightening discussions. This work was supported by NSF Grant Number 92-06023.



## REFERENCES

- [1] see, e.g., D. Pines, *Physica* **199-200**, 300 (1994); D. J. Scalapino, to be published in *Physics Reports*.
- [2] D. A. Wollman *et al.*, *Phys. Rev. Lett.* **71**, 2134 (1993); A. G. Sun *et al.*, *ibid.* **72**, 2267 (1994); P. Chaudhari and S.-Y. Lin, *ibid.* **72**, 1048 (1994); C. C. Tsuei *et al.*, *ibid.* **73**, 593 (1994); A. Mathai *et al.*, preprint.
- [3] P. Hirschfeld and N. Goldenfeld, *Phys. Rev. B* **48**, 4219 (1993); F. Gross *et al.*, *Z. Phys. B* **64**, 175 (1986).
- [4] T. P. Devereaux *et al.*, *Phys. Rev. Lett.* **72**, 396 (1994); *Phys. Rev. B* **50**, 10287 (1994).
- [5] We assume here that the scattering occurs predominantly within the anti-bonding Cu-O band, which has the largest density of states and curvature at the Fermi level (see Eq. (2)). The neglect of interband scattering (see M. Krantz and M. Cardona, *Phys. Rev. Lett.* **72**, 3290 (1994) but also T. P. Devereaux *et al.*, *Phys. Rev. Lett.* **72**, 3291 (1994)) is also motivated from the uniformity of the Raman response measured in *all* the cuprates, regardless of the different band structures.
- [6] See, e.g., P. J. Hirschfeld, P. Wölfle, and D. Einzel, *Phys. Rev. B* **37**, 83 (1988).
- [7] K. Ueda and T. M. Rice, in *Theory of Heavy Fermions and Valence Fluctuations*, edited by T. Kasuya and T. Saso (Springer, Berlin, 1985); L. P. Gorkov, *Pis'ma Zh. Eksp. Teor. Fiz.* **40**, 351 (1994) [*Sov. Phys. JETP* **40**, 1155 (1985)].
- [8] L. S. Borkowski and P. J. Hirschfeld, *Phys. Rev. B* **49**, 15404 (1994).
- [9] T. Staufer *et al.*, *Phys. Rev. Lett.* **68**, 1069 (1992).
- [10] R. Nemetschek *et al.*, *Phys. Rev. B* **47**, 3450 (1993).
- [11] A linear rise of the  $B_{1g}$  spectrum has been observed in clean YBCO samples for a larger range of frequencies [see e.g. X. K. Chen *et al.*, *Phys. Rev. B* **48**, 10530 (1993)]. It

has been shown that this may be due in part to the Fano distortion of  $B_{1g}$  phonon  $\sim 340\text{cm}^{-1}$  which couples to the electronic continuum [T. P. Devereaux, A. Virosztek, and A. Zawadowski, Phys. Rev. B (in press)].

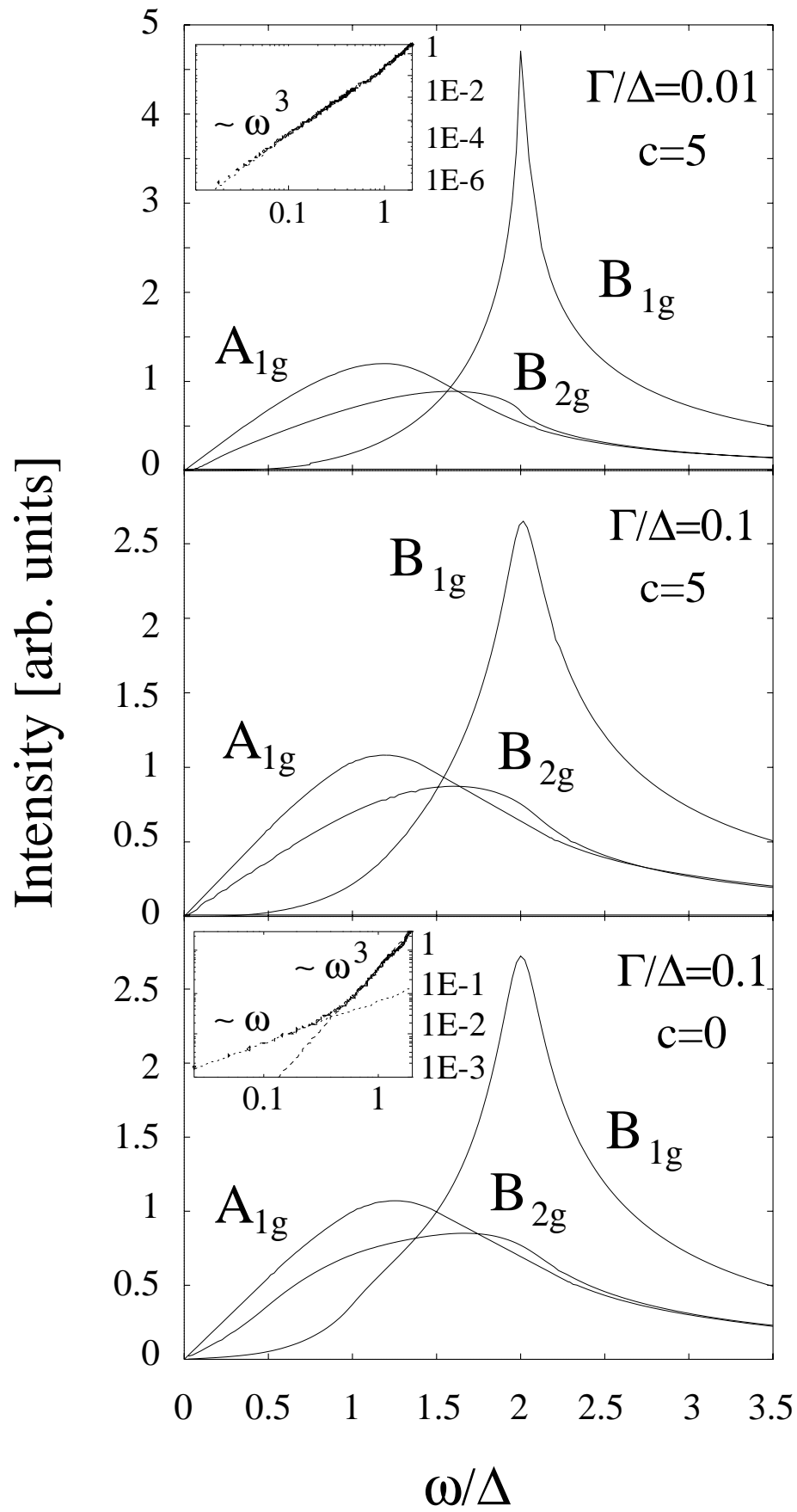
- [12] S. L. Cooper *et al.*, Phys. Rev. B **38**, 11934 (1988); T. Staufer *et al.*, Solid State Commun. **75**, 975 (1990); F. Slakey *et al.*, Phys. Rev. B **39**, 2781 (1991).
- [13] A. Zawadowski and M. Cardona, Phys. Rev. B **42**, 8798 (1990); T. P. Devereaux, Phys. Rev. B **45**, 12965 (1992).
- [14] C. M. Varma *et al.*, Phys. Rev. Lett. **63**, 1068 (1990); B. S. Shastry and B. I. Shraiman, Int. Journ. of Mod. Phys. B **5**, 365 (1991); F. Slakey *et al.*, Phys. Rev. B **43**, 3764 (1991).
- [15] A. Virosztek and J. Ruvalds, Phys. Rev. Lett. **67**, 1657 (1991).
- [16] T. Moriya *et al.*, J. Phys. Soc. Jpn. **52**, 2905 (1990); A. Sokol and D. Pines, Phys. Rev. Lett. **71**, 2813 (1993).

## FIGURES

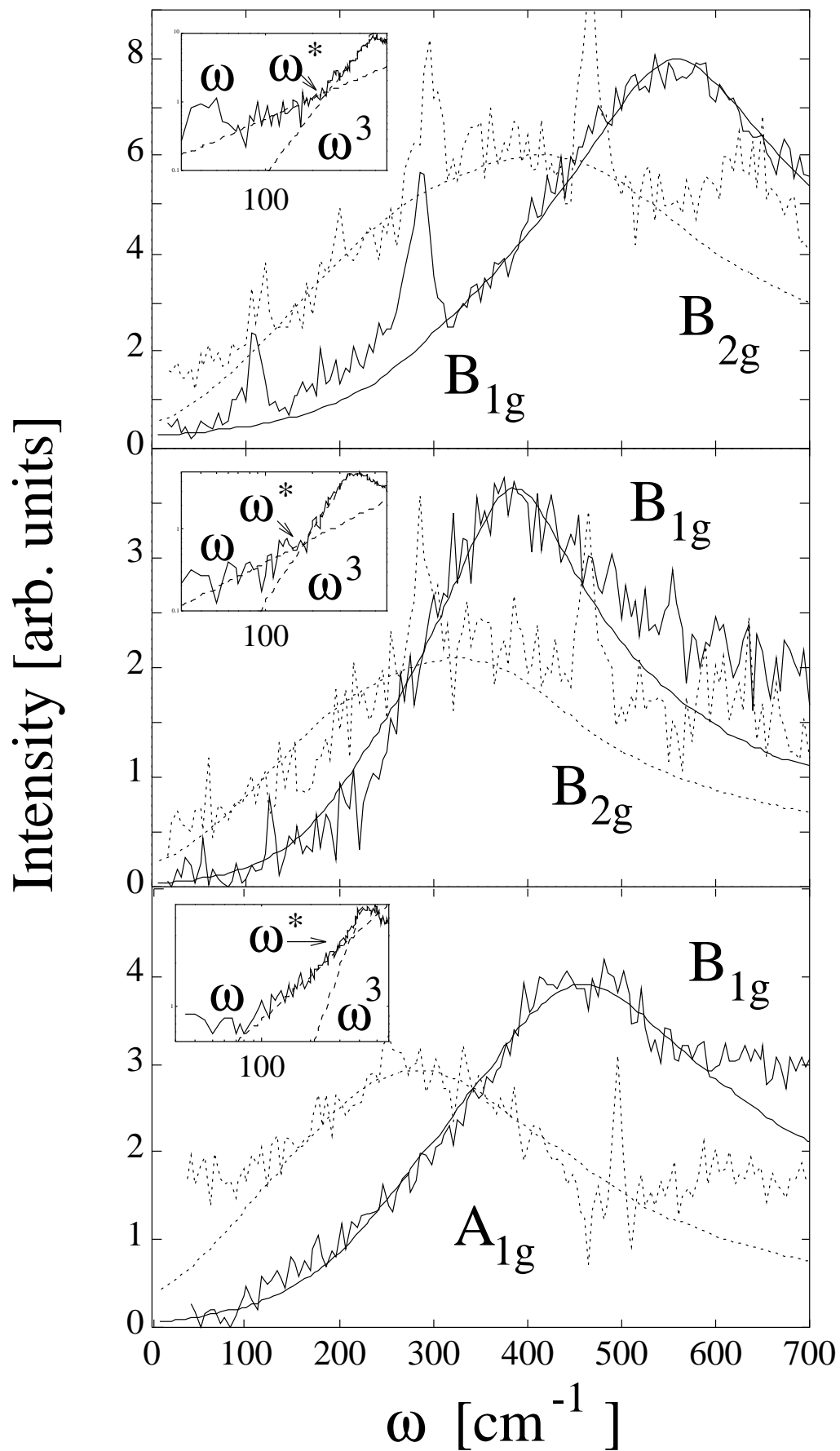
FIG. 1. Raman spectra for  $B_{1g}$ ,  $B_{2g}$ , and  $A_{1g}$  channels, with values of  $c$  and  $\Gamma$  indicated. Magnitude of the Raman vertices are set to 1. The inset shows the low frequency behavior of the  $B_{1g}$  channel. For the case of resonant scatterers ( $c = 0$ , bottom panel), the low frequency behavior crosses over from  $\omega$  to  $\omega^3$ .

FIG. 2. Fit to the data taken for the  $B_{1g}$  and  $B_{2g}$  channels in as-grown Bi 2:2:1:2 ( $T_c = 86K$ , top panel),  $O_2$  annealed Bi 2:2:1:2 ( $T_c = 79K$ , middle panel) and for the  $B_{1g}$  and  $A_{1g}$  channels in Tl 2:2:0:1 ( $T_c = 80K$ , bottom panel) obtained in Refs. [9] and [10]. The phonon contributions have been subtracted out in the middle and bottom panels. The parameters used are  $\Delta_0 = 287, 190$ , and  $240 \text{ cm}^{-1}$ ,  $\Gamma/\Delta_0 = 0.125, 0.2$ , and  $0.25$ , for the top, middle, and bottom panels, respectively. Inset: Log-log plot of the low frequency portion of the  $B_{1g}$  response. The crossover frequency  $\omega^*/\Delta_0 = 0.38, 0.47$ , and  $0.73$  for the top, middle, and bottom panels, respectively.

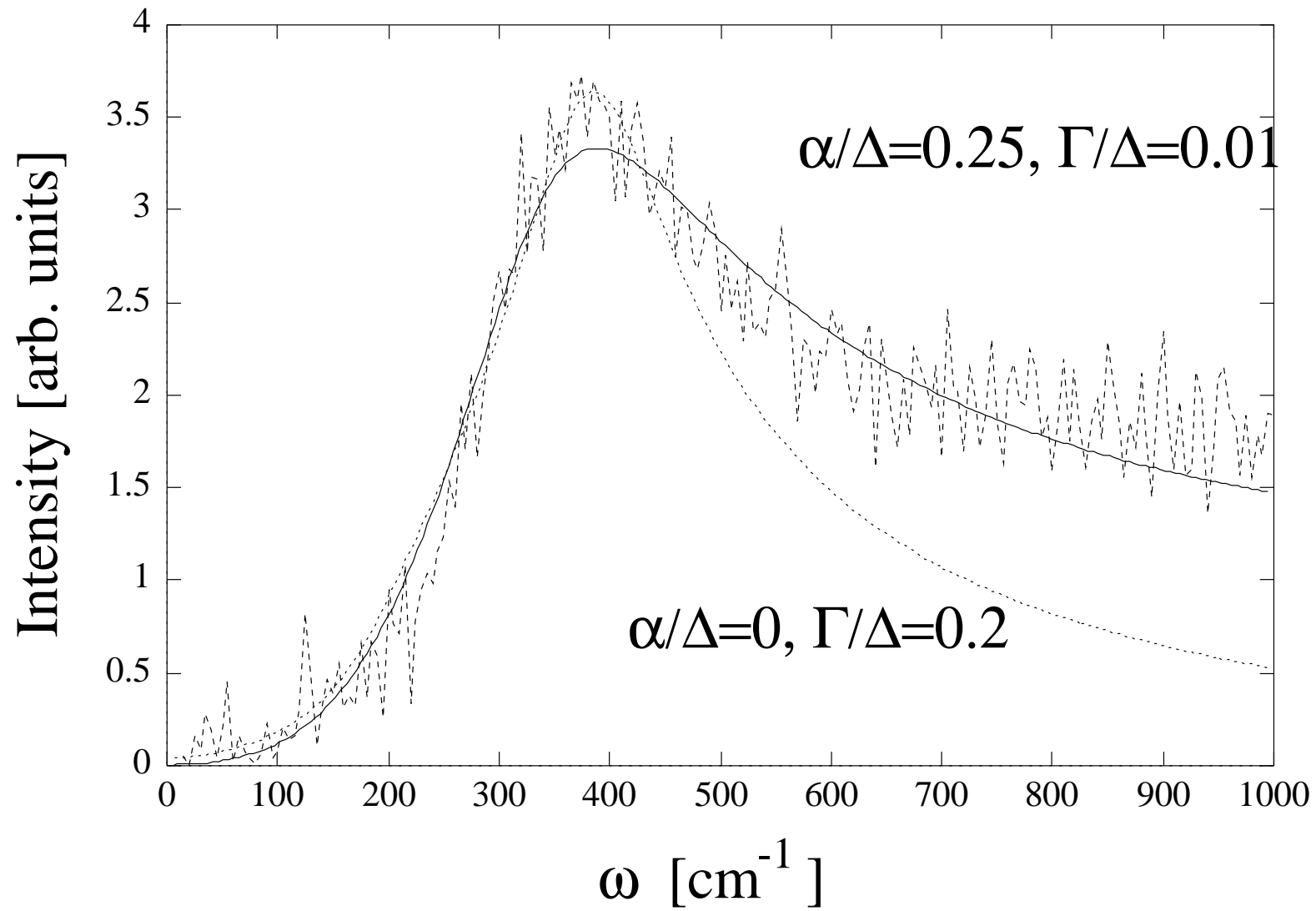
FIG. 3. Theory curves calculated with and without interaction self energy, Eq. 7, compared to the Raman spectrum for the  $B_{1g}$  channel of the  $O_2$ - annealed Bi 2:2:1:2 sample. The dotted line is redrawn from Fig. 2.



Devereaux, Fig. 1



Devereaux Fig. 2



Devereaux, Fig. 3